X- and Y-Cells in the Dorsal Lateral Geniculate Nucleus of the Owl Monkey (Aotus trivirgatus)

Author(s): S. Murray Sherman, J. R. Wilson, J. H. Kaas and S. V. Webb

Source: *Science*, New Series, Vol. 192, No. 4238 (Apr. 30, 1976), pp. 475-477
Published by: American Association for the Advancement of Science
Stable URL: https://www.jstor.org/stable/1741358
Accessed: 07-08-2019 18:11 UTC

X- and Y-Cells in the Dorsal Lateral Geniculate Nucleus of the Owl Monkey (*Aotus trivirgatus*)

Abstract. *The owl monkey, as do other mammals, has X- and Y-cells in its lateral geniculate nucleus. X-cells are found in the parvocellular laminae; Y-cells, in the magnocellular laminae.*

Studies of the cat retino-geniculo-cortical system have recently defined at least two parallel and functionally distinct pathways involving X- and Y-cells, respectively (*1–3*). Preliminary data have extended this arrangement to the tree shrew (*4*), but to our knowledge no clear evidence for X- and Y-cells has yet been presented for primates (*5*). We now extend this general scheme to the owl monkey (*Aotus trivirgatus*) with the identification of X- and Y-cells in its lateral geniculate nucleus. Figure 1 shows the layering scheme in this nucleus (*6*). Not only did we find that the vast majority of neurons in the lateral geniculate nucleus was clearly composed of either X- or Y-cells, but we also found only X-cells in the parvocellular laminae and only Y-cells in the magnocellular laminae (see Fig. 1).

We studied electrophysiological properties from 59 single geniculate neurons in four monkeys and used techniques essentially identical to previously reported methods (*2, 4*). Monkeys were anesthetized (initially with halothane, then maintained with N_2O/O_2, 70/30), paralyzed and artificially ventilated, and end-tidal CO_2 was monitored and kept near 3 to 4 percent. The pupils were dilated with topical atropine, and contact lenses were chosen by retinoscopy to focus the eyes on a 114-cm-distant tangent screen.

Stimulating electrodes were placed in the optic chiasm and at various sites throughout the striate cortex. Action potentials from single geniculate neurons were extracellularly monitored with varnished tungsten microelectrodes (10 to 20 megohms at 500 hertz). We used black or white targets against the gray tangent screen to plot and study neuronal receptive fields. Colored stimuli were not used in these experiments. For many cells, post-stimulus histograms relating firing rate to various stimulus parameters [see (*7*) and Fig. 2] were generated by use of an optical system controlled by a computer. Cells were classified as X- or Y-cells by previously described methods based on axonal conduction velocity and receptive field criteria (*2, 4*).

We studied each cell for the following properties (*2, 4*): (i) action potential latencies for orthodromic optic chiasm stimulation and, where possible, antidromic cortical stimulation; (ii) the dominant eye for receptive field activation; (iii) the size of the field center; (iv) the duration for which the neuron responded above spontaneous levels while a stimulus of appropriate contrast (that is, white for ON center and black for OFF center) was held in the field center; and (v) whether or not the cell was excited by rapidly moving (> 100° per second) large targets of appropriate contrast to excite the cell through its antagonistic surround (that is, black for ON center and white for OFF center). After the recording sessions, the monkeys' brains were histologically prepared in order to reconstruct electrode penetrations and cell locations (see Fig. 1).

Nearly all of the cells were classified as either X-cells (42 of 59; 71 percent) or Y-cells (15 of 59; 25 percent). Only two of 59 cells (3 percent) were unclassified. We also sampled three Y-fibers apparently in the optic radiation plus two X- and seven Y-fibers in the optic tract (*8*). As in the cat and tree shrew (*1, 2, 4*), X-cells compared to Y-cells in the owl monkey displayed more tonic or sustained responses to appropriate standing contrast (Fig. 2A), poor activation by fast visual stimuli (Fig. 2B), and no activation by fast targets of appropriate contrast to excite the cell through the surround. The difference between X- and Y-cells based on the tonic-phasic distinction was particularly dramatic in the owl monkey. All but two X-cells sustained their response to an appropriate, centered target for as long as it was presented (30 to 50 seconds) whereas no Y-cell responded for more than 1 or 2 seconds to such a stimulus, and most Y-cell responses were considerably briefer (see Fig. 2A). Field center sizes and latencies to electrical stimulation for these geniculate neurons were also similar to analogous data for X- and Y-cells from the cat and tree shrew (*1, 2, 4*). For 42 X-cells, the field sizes averaged 0.3° ± 0.1° (mean and standard deviation for this and the following values); for 15 Y-cells this was 0.9° ± 0.3°. Latencies to orthodromic optic chiasm stimulation for 28 X-cells averaged 2.3 ± 0.3 msec; for 12 Y-cells this was 1.4 ± 0.2 msec. Latencies to antidromic cortical stimulation for 14 X-cells averaged 2.3 ± 0.5 msec; for eight Y-cells this was 1.5 ± 0.2 msec.

In addition to finding clearly distinguishable geniculate X- and Y-cells in the owl monkey, we also found these cell types to be anatomically segregated in the nucleus. Figure 1 is a typical example of one of our electrode track reconstructions. Six X-cells were located in the parvocellular laminae, an unclassified neuron was found in the interlaminar zone, and three Y-cells were recorded in the magnocellular laminae. In *every* electrode penetration through the nucleus we noticed the following pattern: first (in the parvocellular laminae) we found neurons with unambiguous X-cell characteristics; then (in the interlaminar zone) we found very few cells (apparently only two in the entire series) which could be isolated above background "hash," and these were unclassified cells; then (in the magnocellular laminae) we found neurons with clear Y-cell features; and finally, we occasionally isolated an optic tract fiber.

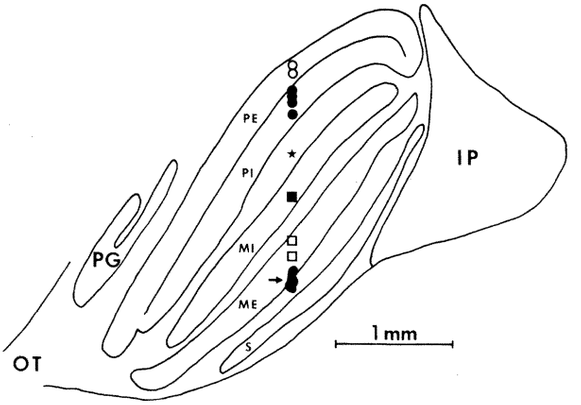

Fig. 1. Reconstruction of electrode penetration through the lateral geniculate nucleus, which is shown in parasagittal section. Closed symbols represent the location of neurons driven by the ipsilateral eye; open symbols, those driven by the contralateral eye; and the lesion is marked by an arrow. Circles represent X-cells; squares, Y-cells; and the star, an unclassified cell. Note that X-cells were in the parvocellular laminae, Y-cells were in the magnocellular laminae, and the unclassified cell was in the cell-poor interlaminar zone (*6*). Abbreviations: *OT*, optic tract; *PG*, perigeniculate; *IP*, inferior pulvinar; *PE*, external parvocellular lamina; *PI*, internal parvocellular lamina; *MI*, internal magnocellular lamina; *ME*, external magnocellular lamina; *S*, lamina *S*.

We have not yet clearly isolated a neuron from lamina *S*, but some of the Y-cells may have been located there, and, indeed, some of the X- and Y-cells may have been located in the interlaminar zone separating the X- and Y-cell populations.

Therefore, as in the cat and tree shrew, the lateral geniculate nucleus in the owl monkey has neurons which can be classified as X-cells or Y-cells. Compared to the geniculate Y-cells, in all three animals the geniculate X-cells receive more slowly conducting retinal afferents and project more slowly conducting axons to striate cortex. Based on this preliminary evidence, then, the owl monkey, as well as the cat and tree shrew, apparently has substantially distinct, parallel X- and Y-pathways from retina through the lateral geniculate nucleus to striate cortex. It is tempting to extrapolate this scheme of parallel processing to many other mammals, including other primates. Finally, we have found that in the owl monkey, the parvocellular laminae contain X-cells; the magnocellular, Y-cells (*9*). Perhaps a similar anatomical division applies to other primates, including man.

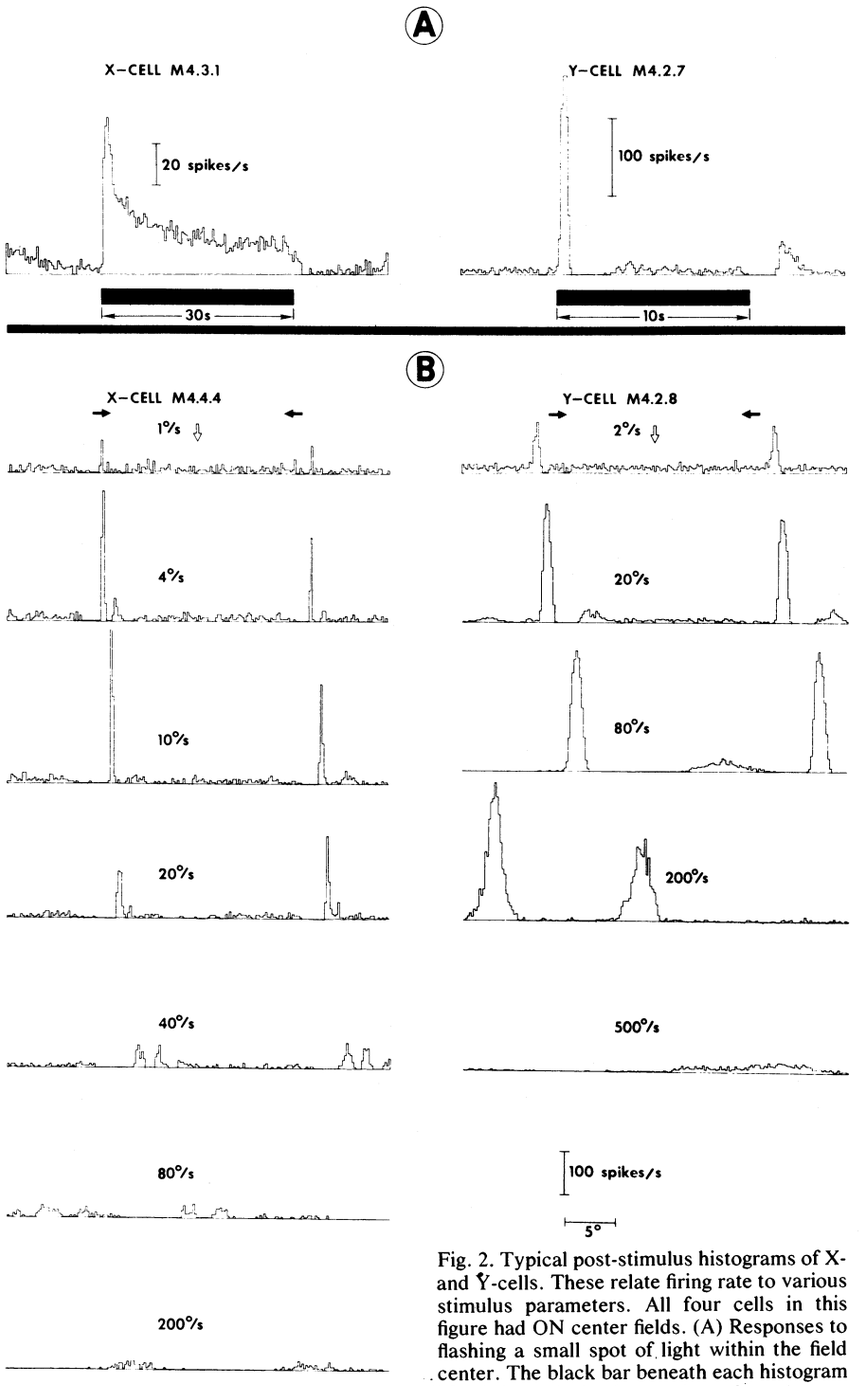

Fig. 2. Typical post-stimulus histograms of X- and Y-cells. These relate firing rate to various stimulus parameters. All four cells in this figure had ON center fields. (A) Responses to flashing a small spot of light within the field center. The black bar beneath each histogram indicates when the light was presented. The X-cell fired above the background rate for as long as the stimulus was in the field, whereas the Y-cell fired above the background rate for less than 0.5 second after the stimulus onset. (B) Responses to slits of light (0.5° × 7°) moved broadside through the fields at various speeds. Speeds are indicated for each histogram. The stimulus was moved left-to-right during the first half of each histogram, then turned around to move right-to-left during the second half. These features are indicated by arrows at the top of each column: the solid arrows indicate direction of stimulus movement; and the open arrows, the stimulus turnaround point. Clear responses in the X-cell ceased at speeds above 40° or 80° per second, while the Y-cell responded clearly at speeds greater than 200° per second. Note that at higher speeds, each response appeared later in the histogram. This obtained because the histogram bin widths are shorter in duration at higher speeds, and with a constant latency from stimulus to response, the response would thus fall into later bins at higher speeds. Abbreviation: s, second.

S. MURRAY SHERMAN
J. R. WILSON
Department of Physiology, University of Virginia School of Medicine, Charlottesville 22901
J. H. KAAS
Department of Psychology, Vanderbilt University, Nashville, Tennessee 37240
S. V. WEBB
Department of Physiology, University of Virginia School of Medicine, Charlottesville 22901

References and Notes

1. C. Enroth-Cugell and J. G. Robson, *J. Physiol. (London)* **187**, 517 (1966); B. G. Cleland, M. W. Dubin, W. R. Levick, *ibid.* **217**, 473 (1971); J. Stone and B. Dreher, *J. Neurophysiol.* **36**, 551 (1973).
2. K.-P. Hoffmann, J. Stone, S. M. Sherman, *J. Neurophysiol.* **35**, 518 (1972).
3. Recent studies have also identified a third cell type (the W-cell) in the retina and lateral geniculate nucleus of the cat, and this may represent a third parallel pathway. For details, see P. D. Wilson and J. Stone, *Brain Res.* **92**, 472 (1975), and B. G. Cleland, R. Morstyn, H. G. Wagner, W. R. Levick, *ibid.* **91**, 306 (1975).
4. S. M. Sherman, T. T. Norton, V. A. Casagrande, *ibid.* **93**, 152 (1975).
5. Other studies of monkey retina and lateral geniculate nucleus have shown axonal conduction velocity groupings reminiscent of X- and Y-cells, but no systematic attempt was made to classify the neurons as X- or Y-cells. For example, see P. Gouras, *J. Physiol. (London)* **204**, 407 (1969), and R. T. Marroco and J. B. Brown, *Brain Res.* **92**, 137 (1975).
6. J. H. Kaas, R. W. Guillery, J. M. Allman, *Brain Behav. Evol.* **6**, 253 (1972).
7. P. O. Bishop, J. S. Coombs, G. H. Henry, *J. Physiol. (London)* **219**, 625 (1971).
8. Units were classified as optic radiation fibers if they had a fiber-like action potential and were located well dorsal to the known geniculate position; otherwise, their electrophysiological properties were indistinguishable from those of geniculate cells. Optic tract fibers were classified on the basis of wave form and the nature of their response to optic chiasm stimulation: action potentials followed such stimulation at high frequencies (> 200 hertz) with no detectable latency variation.
9. Anatomical data from the rhesus monkey suggest a less clear distinction. A. H. Bunt, A. E. Hendrickson, J. S. Lund, R. D. Lund, and A. F. Fuchs [*J. Comp. Neurol.* **164**, 265 (1975)] suggested that all retinal ganglion cells project to the parvocellular laminae, whereas only the larger ones project to the magnocellular laminae. They thus concluded that W-, X-, and Y-cells (*1–3*) project to the parvocellular laminae,

and perhaps only Y-cells project to the magnocellular laminae. While our electrophysiological data support their latter conclusion, we found no evidence for W- or Y-cell input to the parvocellular laminae. If owl and rhesus monkeys share a common retino-geniculate pattern, this is an apparent noncorrespondence between anatomical and physiological observations of the parvocellular laminae, and it cannot yet be explained.

10. This research was supported by PHS grants EY 01565 and EY 12377. Also, S.M.S. was supported by research career development award EY 00020 from PHS. We are grateful to Dr. Leon Schmidt, Southern Research Institution, Birmingham, Alabama, for providing the owl monkeys used in this study.

12 January 1976

Dendritic Reorganization of an Identified Motoneuron During Metamorphosis of the Tobacco Hornworm Moth

Abstract. *In the tobacco hornworm, many larval motoneurons become respecified and supply new muscles in the adult. Changes in the morphology of one such neuron were examined through metamorphosis. The dendritic pattern of the adult comes about both by outgrowth from the primary and secondary branches of the larval neuron and by the development of new branches that are unique to the adult.*

Since the classic studies of Lyonet (*1*) over 200 years ago, it has been known that "complete" metamorphosis of insects is accompanied by an extensive reorganization of the nervous system. In examining these changes, a number of investigators have concluded that at least part of the adult system is constructed from preexisting larval neurons (*2, 3*). Thus, differentiated larval neurons must redifferentiate during metamorphosis and assume new functions in the adult. We report that in an identified motoneuron this change in function is accompanied by an extensive alteration of the dendritic morphology. We also examined the extent to which the larval structures of the neuron contribute to the final adult form.

In adult *Manduca sexta*, 89 percent of the motoneurons in the fourth abdominal ganglion (ganglion A_4) are derived from motoneurons that were present in the larva (*3*). Since the larva and adult show extreme differences in the musculature of segment A_4, it was apparent that some neurons must innervate different muscles and consequently have different functions in these two stages. Male last instar larvae, diapausing pupae, and pharate (*4*) adults were used. Possible changes in dendritic morphology of motoneurons were examined by back diffusion of $CoCl_2$ through the proximal stump of peripheral nerves (*3, 5*) into ganglion A_4. The cobalt served to impregnate the neurons that sent axons out of the respective nerves. After precipitation of the cobalt with ammonium sulfide (*5*), ganglia were fixed in alcoholic Bouin's solution, dehydrated, embedded in paraffin, and serially sectioned at 10 μm. The cobalt was then intensified by silver precipitation according to a modification of Timm's method (*6*). In favorable preparations this procedure revealed dendritic twigs down to 0.5 μm in diameter. Portions of the neuron on each section were traced by using a Leitz drawing tube and a 40 × planar objective and subsequently assembled into a two-dimensional reconstruction of the particular neuron.

The main trunk of the dorsal nerve (*7*) of ganglion A_4 was filled from beyond the second branch. In the pupal and adult stages this procedure filled only two neurons that had their cell bodies and dendritic areas in A_4. Motoneuron MN1 [numbering system according to (*3*)] had a contralateral cell body situated in the ventral lateral region of A_4, anterior to the entry of the other dorsal nerve. A second motoneuron (MN4) had a ventral midline cell body and an axon that divided and sent branches out through both dorsal nerves. Similar staining of larval ganglia revealed a third neuron (MN6). This neuron, which subsequently degenerates during metamorphosis (*3*), had an ipsilateral cell body situated in the dorsomedial region of A_4. Since MN1 had the only large cell body in the ventral lateral region of ganglion A_4 anterior to the dorsal nerve, it was chosen for study. Two other neurons in the larva and only one other neuron in the pupa and adult filled from beyond the second branch of the dorsal nerve, so the dendritic structure of MN1 was not obscured by the branching of many other neurons.

The fact that a neuron with a large cell

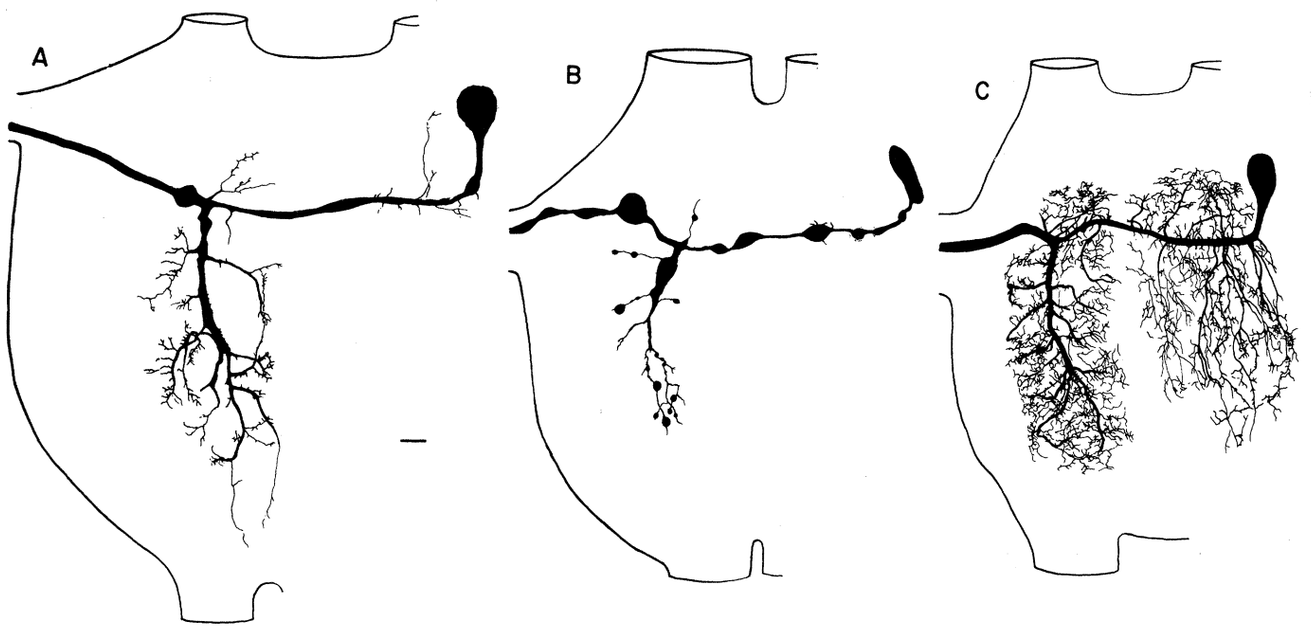

Fig. 1. Dorsal view of a reconstruction of MN1 in the fourth abdominal ganglion of *Manduca sexta*; (A) larva, (B) diapausing pupa, and (C) pharate adult. Scale bar, 20 μm.